Theoretical Population Biology 96 (2014) 20–29

Contents lists available at ScienceDirect

Theoretical Population Biology

journal homepage: www.elsevier.com/locate/tpb

# Coexistence of productive and non-productive populations by fluctuation-driven spatio-temporal patterns

Hilla Behar [a], Naama Brenner [b], Yoram Louzoun [a,*]

[a] Department of Mathematics and Gonda Brain Research Center, Bar-Ilan University, Ramat Gan, Israel
[b] Department of Chemical Engineering and Network Biology Research Lab, Technion, Haifa, Israel

ARTICLE INFO

*Article history:*
Received 9 February 2014
Available online 21 July 2014

*Keywords:*
Stochastic processes
Microorganism population
Microbial cooperation
Coexistence
Spatio-temporal patterns

ABSTRACT

Cooperative interactions, their stability and evolution, provide an interesting context in which to study the interface between cellular and population levels of organization. Here we study a public goods model relevant to microorganism populations actively extracting a growth resource from their environment. Cells can display one of two phenotypes — a productive phenotype that extracts the resources at a cost, and a non-productive phenotype that only consumes the same resource. Both proliferate and are free to move by diffusion; growth rate and diffusion coefficient depend only weakly phenotype. We analyze the continuous differential equation model as well as simulate stochastically the full dynamics. We find that the two sub-populations, which cannot coexist in a well-mixed environment, develop spatio-temporal patterns that enable long-term coexistence in the shared environment. These patterns are purely fluctuation-driven, as the corresponding continuous spatial system does not display Turing instability. The average stability of coexistence patterns derives from a dynamic mechanism in which the producing sub-population equilibrates with the environmental resource and holds it close to an extinction transition of the other sub-population, causing it to constantly hover around this transition. Thus the ecological interactions support a mechanism reminiscent of self-organized criticality; power-law distributions and long-range correlations are found. The results are discussed in the context of general pattern formation and critical behavior in ecology as well as in an experimental context.



## 1. Introduction

Cooperative behavior of individuals in nature has attracted the interest of scientists for many years (Axelrod and Hamilton, 1981; Michod and Roze, 2001; Nowak, 2006). The evolution and stability of cooperation is sometimes formulated as a dilemma or conflict between the optimal strategy of the individual and that of the population. More generally, cooperative interactions and their stability provide a fascinating context in which to investigate the relations between these two levels of organization — the individual and the population. Indeed, a biological population is more than a collection of individuals: it is characterized by its interactions — direct and indirect, by its memory through inheritance, and by its relation with the environment (Moore et al., 2013; Stolovicki and Braun, 2011). Therefore, phenomena at the population level, including evolutionary dynamics and long-term stability of individual traits, are necessarily affected by all these ingredients.

Populations of microorganisms provide a valuable model system to study cooperative interactions. Much is known about the mechanisms underlying microbial cooperative behavior: mutations, gene expression and other processes affect cellular behavior, which in turn affects the environment and feeds back on the individual dynamics (Kummerli et al., 2009; Elhanati et al., 2011). Thus these systems offer concrete test cases for many fundamental issues at the intersection between the individual, the population and the environment. Microbial populations have the great advantage of allowing controlled experiments, where predictions can be tested quantitatively; at the same time the detailed biological knowledge about the processes involved places severe constraints on the models relevant to these systems (Schuster et al., 2010; Damore and Gore, 2012). Indeed previous work has shown that conclusions drawn on fundamental problems may depend subtly on details of realization of the particular biological system. In the present work we focus on models appropriate for microbial interactions taking into account carefully the constraints that they pose.

* Corresponding author.
*E-mail addresses:* hilla.behar2@gmail.com (H. Behar), nbrenner@tx.technion.ac.il (N. Brenner), louzouy@math.biu.ac.il, ylouzoun@gmail.com (Y. Louzoun).

http://dx.doi.org/10.1016/j.tpb.2014.06.002
0040-5809/

One important type of cooperative interaction is induced by the production of public goods: in a population inhabiting a shared environment, individuals depend on a resource for their growth or survival. The resource can be produced or actively extracted from the environment by the individuals, generally at some cost. Once produced, it is shared by other population members as well, thus defining a setting with some degree of cooperation. The more general problem known as public goods cooperation has been considered in several different contexts, from abstract game theory in which encounter rules are defined (Hauert et al., 2006, 2008), through theoretical evolutionary models (Doebeli et al., 2004) and to biophysical aspects of microorganism model systems that secrete resource-extracting molecules outside the cell boundaries (Craig Maclean and Brandon, 2008; Gore et al., 2009; Kummerli et al., 2009; Velicer and Vos, 2009). In general it is by now well established that various mechanisms at the population level can break the symmetry between producers and non-producers, supporting privileged share of the resource to the productive individuals, or inducing assortment of sub-populations, thus enabling coexistence of productive and non-productive phenotypes in the same environment (Nowak, 2006; Damore and Gore, 2012). Spatial structure and mobility, for example, is one such mechanism that has a strong effect on the public goods problem in its various levels of abstraction (Hamilton, 1971; Eshel, 1972; Nowak et al., 1994; Irwin and Taylor, 2001; Perc et al., 2013). Intuitively, when cells are proliferating in different regions in space, and if the cooperative trait is inherited, then it will be directed mainly towards other cooperators. However, different mechanisms can support coexistence in a spatially extended environment and, once again, their fundamental nature may depend on the details of the system.

Previous work on spatial public goods dynamics has focused on a class of models derived from the public goods game in economy, where a well-defined group interacts by individual contribution and a reward common to the group (Wakano, 2007; Wakano et al., 2009; Wakano and Hauert, 2011). This model was transformed to partial differential equations and coexistence was found in one of two possible cases: (A) coexistence already emerges in the mean field ordinary differential equation (ODE); (B) there is no coexistence in the mean field, but a Turing instability in the spatial model described by partial differential equations (PDE) induces spatial patterns of coexistence. In this case, as is typical of the Turing mechanism, the diffusion coefficients of the producers and non-producers must differ greatly (Wakano and Hauert, 2011).

In the context of microbial populations there is no biological justification to assume a difference in diffusion coefficient between different physiological states or even different strains of the same organism. Thus, an argument is needed for the more general case, where diffusion is not strongly dependent on the production of common goods, and where co-existence is impossible in the mean field. We here present and study such a model, which is quite generally suited for microbial populations actively extracting a growth resource from the environment.

In a well-mixed environment with homogeneous interactions, the model exhibits an extreme "tragedy of the commons" scenario: non-productive individuals have a higher fitness, take over the population, and cause extinction due to the extreme dependence of growth on the extracted resource. This is the only fixed point of the well-mixed system, sharpening the question of rescue from the tragedy of extinction. The model has been proposed and studied previously in the presence of strategy changes induced by gene expression, either random or by environmental feedback; then, coexistence can be stabilized in a well-mixed system (Elhanati et al., 2011). Here we resort to the basic resource-extraction dynamics without change of strategy, but in the presence of spatial and demographic fluctuations.

Embedding the populations in space in a continuous dynamical system description with diffusion does not induce non-homogeneous solutions; namely, there is no Turing instability (in contrast to other studied systems of spatial public good games (Wakano et al., 2009)). However, we find that when the discrete stochastic nature of the interactions is taken into account, mobility in space and demographic noise drive the system to a solution where spatio-temporal patterns prevail and allow a nontrivial coexistence of the productive and non-productive sub-populations in a large region of parameter space. The mechanism underlying this phenomenon is based on the existence of an absorbing state extinction transition, a slow timescale of competition, and the stochastic dynamics characteristic of a discrete population of cells. We propose an analogy of this mechanism to self-organized criticality and discuss its relation spatio-temporal patterns found in other ecological models.

## 2. Methods

### 2.1. Numerical integration of ODE and PDE

The ODEs were solved numerically using the Matlab fourth-order Runge Kutta (Jameson et al., 1981), as applied in the MATLAB ode45 function assuming non-stiff equations (Hanselman and Littlefield, 1997). The partial differential equations (PDEs) were solved using a fourth-order Runge Kutta on a two-dimensional $100 \times 100$ square lattice, with periodic boundary conditions. The diffusion scheme that was used was a second-order leapfrog scheme (Alexander, 1977).

### 2.2. Stochastic simulation

Monte Carlo simulations of the studied model were performed on a two-dimensional $100 \times 100$ square lattice with periodic boundary conditions. We initiated the reactants at random positions and enacted each reaction separately. We computed at each lattice point the probability of each reaction and performed reactions according to the prescribed probabilities. At high reaction rates, we used a Poisson approximation (Aparicio and Solari, 2001). The simulation updating was asynchronous (i.e. the lattice sites were updated one at a time with a random order). In each time interval (dt) all lattice sites were updated based on the current values in the lattice. The dynamics were simulated for different parameter values. The lattice size used was the two-dimensional $100 \times 100$ unless otherwise noted. The simulation was described in detail in previous publications (Agranovich et al., 2006; Behar et al., 2012; Davidovich and Louzoun, 2013).

## 3. Model presentation

Our model describes a population of microorganisms in an environment that allows growth in principle; however the growth resource is not directly available for the cells to metabolize but rather needs to be actively extracted. This situation is encountered, for example, when complex sugars need to be hydrolyzed by enzyme secretion (Carlson and Botstein, 1982; Jones et al., 1992) or iron needs to be chelated (Hider and Kong, 2010). The cooperative public goods problem is formalized in this context as follows: one type of cell, with a population size $N_P$, produces the growth resource, while the other type, with a population size $N_{NP}$ does not. The two sub-populations consume the resource $C$ and proliferate following resource consumption. It is important that the resource is absolutely essential for growth, as further discussed below. The fitness difference between the two sub-populations is modeled as a lower net death rate of the non-productive type, representing the cost or internal resources invested to create the growth resource $C$.

These definitions create an indirect interaction between the two sub-populations mediated through the environment.

We formulate the public goods game first in terms of ordinary differential equations, where the variables, $N_P, N_{NP}, C$ represent continuous densities of the productive population, non-productive population and growth resource respectively in a well-mixed environment. We imagine that the growth-limiting public good is extracted from some external source, as in the examples of external iron chelation or hydrolization of an external carbon source. This constrains the rate of public good production to be bounded even for high densities of productive population (Elhanati et al., 2011). The differential equations representing the model are then as follows:

$$\begin{cases} \dfrac{dN_{NP}}{dt} = (\alpha(C) - 1)\, N_{NP} \\ \dfrac{dN_P}{dt} = (\alpha(C) - \delta)\, N_P \\ \dfrac{dC}{dt} = \dfrac{\mu N_P}{\nu + N_P} - k\,(\alpha(C)N_{NP} + \alpha(C)N_P)\,. \end{cases} \tag{1}$$

In this system we define the time unit to be the inverse death rate of the non-productive population $N_{NP}$, with no loss of generality. The growth of both population depends on the resource density through the function $\alpha(C)$, an increasing monotonic concave or linear functions of $C$. The advantage of non-producers over producers is expressed through the condition $\delta > 1$ implying a lower net growth rate at all values of $C$. The resource is produced at a rate that depends on the size of the productive population, saturating hyperbolically, with parameters $\mu, \nu$. Values of the parameters used in the simulations are specified in Table 1.

The "tragedy of the commons" is reflected in this dynamical system as it has only one stable fixed point in which the populations both become extinct. This property stems from the fact that the growth resource has no substitute and that in its absence the populations cannot survive. While this property is sometimes too extreme to describe realistic situations, it is theoretically important to consider it in order to distinguish different mechanisms allowing coexistence — different rescue scenarios from the tragedy.

The dynamical system (1) has an additional fixed point in which the productive population $N_P$ sustains itself, and a balance is achieved between resource consumption and production. This fixed point undergoes a bifurcation and disappears if consumption exceeds growth rate (Elhanati et al., 2011). However even in the region where it is stable with respect to the resource, this fixed point is not stable to invasion of the non-productive population $N_{NP}$ (see Appendix A in Supplementary material).

To introduce spatial distribution of the populations and the resource into the model, we first extend the dynamical system (1) to include diffusion terms, resulting in the partial differential equations

$$\begin{cases} \dfrac{\partial}{\partial t}N_{NP} = (\alpha(C) - 1)\, N_{NP} + D_{NP}\nabla^2 N_{NP} \\ \dfrac{\partial}{\partial t}N_P = (\alpha(C) - \delta_2)\, N_P + D_P\nabla^2 N_P \\ \dfrac{\partial}{\partial t}C = \dfrac{\mu N_P}{\nu + N_P} - k\,(\alpha(C)N_{NP} + \alpha(C)N_P) + D_C\nabla^2 C, \end{cases} \tag{2}$$

where all dynamical variables are now functions both of time $t$ and space $\mathbf{r}$: $N_{NP} = N_{NP}(\mathbf{r}, t)$, with $\mathbf{r} = (x, y)$ for two dimensional space. These variables now have also spatial dynamics described by the diffusion operator, in two dimensions $\nabla^2 = \frac{\partial^2}{\partial x^2} + \frac{\partial^2}{\partial y^2}$, and characterized by three respective diffusion coefficients $D_{NP}, D_P, D_C$. It is biologically reasonable that cellular diffusion does not depend strongly on a physiological cell state such as gene expression; we therefore take the diffusion coefficient for both cells to be the same and that of the resource generally different. Numerical integration of these equations shows results similar to those of the non-spatial model in terms of the long-time dynamics: for an initial condition where the populations are of equal size, the non-productive population first increases relative to the productive one and then the system flows towards the state where the two populations become extinct (Fig. C1 in Supplementary material). More generally, one can test for Turing instability around the fixed point by linear stability analysis of the space-extended system. It is found that in the region of parameters where the ODE eigenvalues are negative, so are the PDE eigenvalues and therefore this system does not display Turing instability (see Appendix B in Supplementary material).

**Table 1**
A definition of all parameters in model (1).

| Parameter | Description | Value |
|---|---|---|
| $\alpha(C)$ | The growth rate of the populations | $\alpha(C) = 0.01C$ |
| $\delta$ | The death rate of the population $N_P$ | 1.05 |
| $\mu$ | Maximal production rate of resource by $N_P$ | 110 |
| $\nu$ | Saturation parameter of resource production | 100 |
| $k$ | Inverse yield | 0.5 |

## 4. Stochastic simulations

When the same system is described by discrete stochastic reactions, a completely different type of dynamics emerges. We define the model by a set of discrete stochastic interactions; the variables now represent numbers of cells/molecules instead of densities; the two populations are characterized by the following production and death reactions:

- $NP \xrightarrow{\alpha(c)} NP + NP$
- $NP \xrightarrow{1} \phi$
- $P \xrightarrow{\alpha(c)} P + P$
- $P \xrightarrow{\delta} \phi$,

where $P$ and $NP$ are a single producer and non-producer respectively, and $c$ is a unit of resources. Values above the arrows represent the reaction probabilities per unit time. The resource molecules are produced by the productive population and consumed by both populations also in discrete, stochastic events:

- $P \xrightarrow{\frac{\mu}{\nu+P}} P + c$
- $P + c \xrightarrow{k\alpha(c)} P$
- $NP + c \xrightarrow{k\alpha(c)} NP$.

Finally, diffusion is performed through a random walk of organisms and resources to randomly chosen neighboring sites, with diffusion rates of $D_P$, $D_{NP}$ and $D_C$ respectively.

The mean field description of this system is given by Eq. (1), and the spatial continuous ("reaction–diffusion") approximation by Eq. (2).

We studied this system by running stochastic simulations of the reactions on one and two dimensional lattices. Each lattice site contains a discrete number of cells, thus incorporating the effect of demographic noise. In most of the simulations we took the diffusion coefficient to be equal for the two phenotypes, although this was not essential for obtaining the main results. For more details about the stochastic simulation see Methods.

The results of the simulation show that spatio-temporal patterns develop in the system as illustrated in Fig. 1. Fig. 1(a), (b) show two-dimensional density maps of non-producing 1(a) and producing 1(b) cells for a small cellular diffusion coefficient. These snapshots were taken after 1000 time steps; at this time point

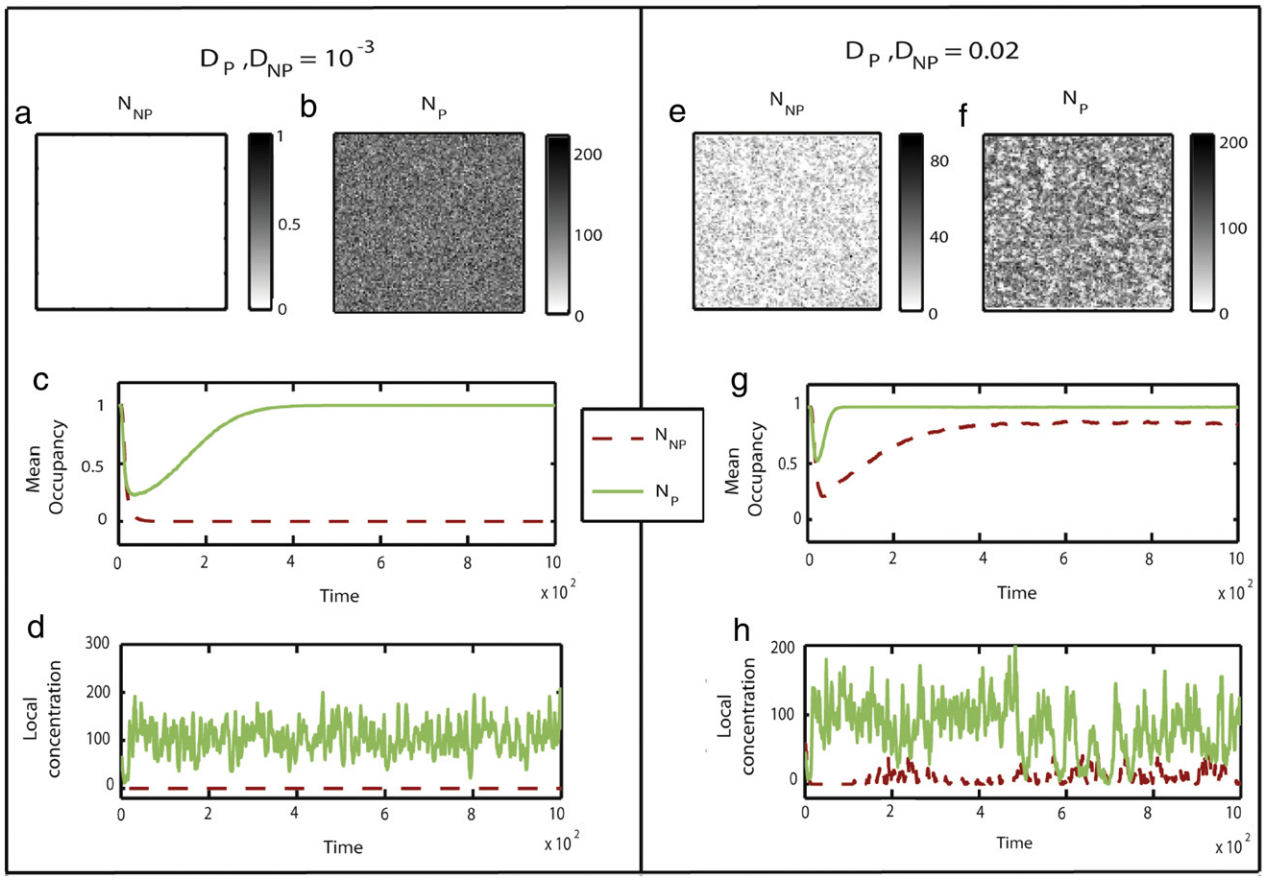


**Fig. 1.** Stochastic simulation results of the spatial model. (a)–(d) Population diffusion coefficients of $D_N = D_{NP} = 10^{-3}$. Snapshots of occupancy map for $N_{NP}$ (a) and $N_P$ (b). (c) Space-averaged occupancy of the populations as a function of time: producing (solid green line) and non-producing (dashed red line). (d) Local concentration in one lattice site as a function of time: producing (solid green line) and non-producing (dashed red line) cells. (e)–(h) Population diffusion coefficients of $D_N = D_{NP} = 2 \cdot 10^{-2}$. Snapshot of $N_{NP}$ (e) and of $N_P$ (f). (g) Space-averaged occupancy as a function of time. (h) Local concentration in one lattice site as a function of time. Parameters used for all simulations: $\alpha(C) = 0.01C$, $\delta = 1.05$, $k = 0.5$, $\mu = 110$, $\nu = 100$, $D_C = 10^{-2}$. (For interpretation of the references to colour in this figure legend, the reader is referred to the web version of this article.)

the average populations have already been stabilized. The non-productive population has become extinct, while the producing one maintains a spatially varying nonzero density. This state was achieved from an initial condition of a mixed population, indicating that it is stable with respect to invasion of non-productive cells. In contrast, Fig. 1(e), (f) show density maps in which both sub-populations are nonzero; thus when the diffusion coefficient is higher, the dynamics, starting from the same initial condition, converges to a state of coexistence. We see that in this simulation, coexistence between producing and non-producing sub-populations is supported for extremely long timescales and is characterized by spatio-temporal patterns, as shown in Fig. 1(e), (f), (h).

The number of cells in each lattice site is not restricted in our model and can take any non-negative integer value. However in order to highlight the question of coexistence, we define the occupancy of each cell type at a lattice site to be 0 if there are no cells of that type and 1 if there are any positive number of cells. The mean occupancy, i.e. the occupancy averaged over all lattice sites (a number between 0 and 1), is plotted in Fig. 1(c), where it is seen that in the long run the system settles into a state with only producing cells whereas the non-producers have become extinct. In contrast, Fig. 1(g) shows the same plot for the higher diffusion coefficient where coexistence can be clearly observed to occur and persists for entire length of the simulation. Inspection of Fig. 1(g), (h) shows that, while a sizable fraction of space is populated by non-producing cells (Fig. 1(g)), there is a non-negligible fraction which carries exactly zero non-producers. Moreover, in mixed sites the non-producers' local population size is typically much smaller than that of the producers; this observation turns out to play an important role in the coexistence mechanism as discussed later.

## 5. Dependence of coexistence on diffusion coefficients

Clearly by Fig. 1 coexistence depends on the populations' (common) diffusion coefficient. To quantify this dependence we plot in Fig. 2 the asymptotic long-time mean occupancy of the two cell types as a function of diffusion coefficient. Fig. 2(a) shows that for a small cellular diffusion coefficient $\left(D_P, D_{NP} < 10^{-2}\right)$, the non-productive population has become extinct in the long run and the productive population survives and takes over the entire space; the mean occupancy of producing cells is 1 and that of non-producing cells is 0. This is the long-time solution whose transient space-averaged dynamics was presented in Fig. 1(c) and a corresponding spatial snapshot in Fig. 1(a), (b). The survival of the producer population in this regime relies on spatial segregation and is similar to a group advantage mechanism (Roberts, 2005; Alexander and Borgia, 1978).

At the other extreme of fast diffusion $\left(D_P, D_{NP} > 4 \cdot 10^{-1}\right)$ the populations will rapidly mix, the produced public good will be shared equally by all and the system will converge to the mean field solution, the empty state. This is seen in Fig. 2(a) as both mean occupancies become zero at the right end of the plot.

An interesting behavior arises in between: if the diffusion coefficient is in an intermediate range $\left(10^{-2} < D_P, D_{NP} < 4 \cdot 10^{-1}\right)$, the two sub-populations can coexist. At the lower end of this regime, the mean occupancy of non-producers increases continuously from zero indicating that in some lattice sites both types

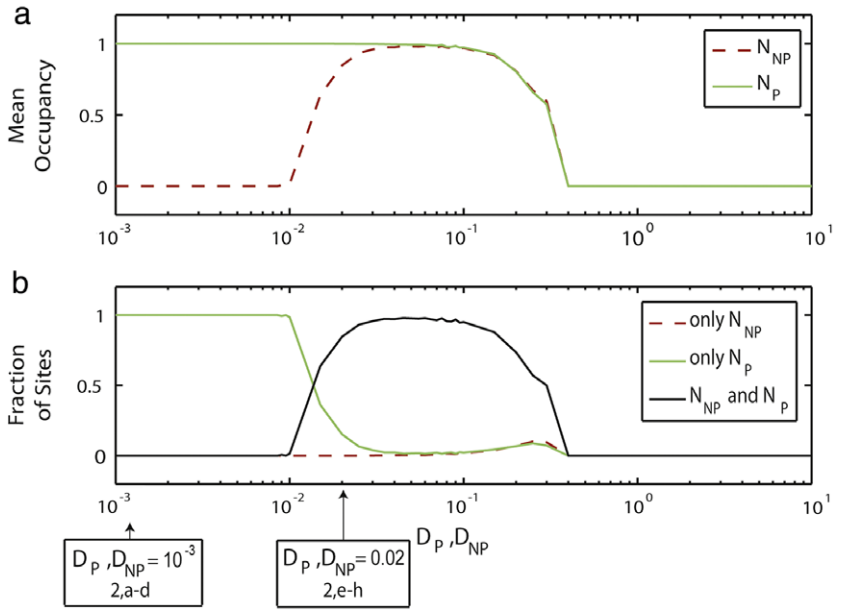


**Fig. 2.** Coexistence depends on the cellular diffusion coefficient. (a) Space-averaged occupancy of $N_{NP}$ (dashed red line) and $N_P$ (solid green line) in stochastic simulation as a function of cellular diffusion coefficient. (b) Percent of the lattice sites with only $N_P$ and no $N_{NP}$ (solid green line), with only $N_{NP}$ and no $N_P$ (dashed red line), and with both $N_P$ and $N_{NP}$ (solid black line). Parameters used for all simulations: $\alpha_1(C) = 0.01C$, $\delta = 1.05$, $k = 0.5$, $\mu = 110$, $\nu = 100$, $D_C = 10^{-2}$. (For interpretation of the references to colour in this figure legend, the reader is referred to the web version of this article.)

coexist locally whereas in others only producers exist. As the diffusion coefficient increases in this regime, both mean occupancies reach one, before decreasing together to zero. Fig. 2(b) shows the fraction of sites in which each sub-population survives separately, showing that generally non-producers cannot populate a site on their own for a long time.

The simulation results presented so far were performed with the same linear growth rate as a function of resource for both sub-populations. However the results are more general; we have repeated the simulations and analysis in a parallel system where the growth rate is a non-linear (Monod) function of the resource, with similar results (Appendix C in Supplementary material).

To understand the behavior across diffusion coefficients, we imagine an initial spatial distribution consisting of separate islands of $N_{NP}$ and $N_P$, as illustrated in Fig. 3(a). Now consider how this configuration will evolve in the presence of diffusion. If the populations are diffusing extremely slowly, one may view each island as practically independent; this situation provides privileged share to the producers because of their clustering and deprives access from the non-producers for the same reason. Therefore, only the productive population $N_P$ can sustain itself in its islands while the non-productive population will become locally extinct, as illustrated in Fig. 3(b). On the longer timescales characteristic of diffusion, those patches in which only producing cells survived will invade the empty regions, resulting in only one possible outcome in the long run: a population of producing cells uniform in space, as illustrated in Fig. 3(c) (see also Fig. 1(a)–(c)).

If the populations are diffusing extremely rapidly, the islands will first mix such that each site contains both cell types. Then the entire population will have the same access to the produced resource and the system will behave as in the mean field: at first non-producers will take over and then both $N_P$ and $N_{NP}$ will become extinct. This scenario is illustrated schematically in Fig. 3(a), (f), (g).

In the regime of intermediate diffusion coefficient, non-producing cells can invade into the producing clusters, but although their growth rate at a given resource concentration is higher, they will not necessarily take over the population and the invasion may fail with high probability. The invasion may still succeed in some regions and cycles of invasion with stochastic outcome can support the long-term spatio-temporal patterns. This is illustrated schematically in Fig. 3(a), (d), (e). A detailed description of this nontrivial scenario is given in the next sections.

## 6. Dependence of coexistence on resource dynamics

How generic is the coexistence in parameter space? To further explore this question we studied the effect of the time scales affecting the dynamics. The two diffusion coefficients and the resource turnover define several important timescales in the problem; this is most clearly seen in nondimensional units. In the case of a linear growth function ($\alpha(C) = \alpha C$), the model takes the scaled form of:

$$\begin{cases} \dfrac{\partial}{\partial t} n_{NP} = (c-1)\, n_{NP} + d_{NP} \nabla^2 n_{NP} \\ \dfrac{\partial}{\partial t} n_P = (c-\delta)\, n_P + d_P \nabla^2 n_P \\ \dfrac{\partial}{\partial t} c = \tilde{\mu} \left[ \dfrac{n_P}{\tilde{\nu} + n_P} - (n_{NP} + n_P)\, c \right] + d_c \nabla^2 c \end{cases} \tag{3}$$

with

$$n_{NP} = \frac{k}{\mu} N_{NP}; \qquad n_P = \frac{k}{\mu} N_P; \qquad c = \alpha C; \qquad \tilde{\mu} = \alpha \mu;$$

$$\tilde{\nu} = \frac{k}{\mu} \nu; \qquad d_{NP} = D_{NP}; \qquad d_P = D_P; \qquad d_c = D_C.$$

From these equations the stochastic dimensionless systems is derived in the same way as in Section 4. Varying the diffusion coefficients or the resource turnover rate $\tilde{\mu}$ has no effect on the stability of the mean field continuous system, but has a crucial effect on the stability of the stochastic system, as already seen in the previous section. In order to display the effect of all three timescales on the problem, Fig. 4 shows several two-dimensional coexistence maps as a function of the two diffusion coefficient, each corresponding to a different value of $\tilde{\mu}$. White areas represent coexistence, gray areas represent survival of only the productive population, and black areas represent regions of parameters where the

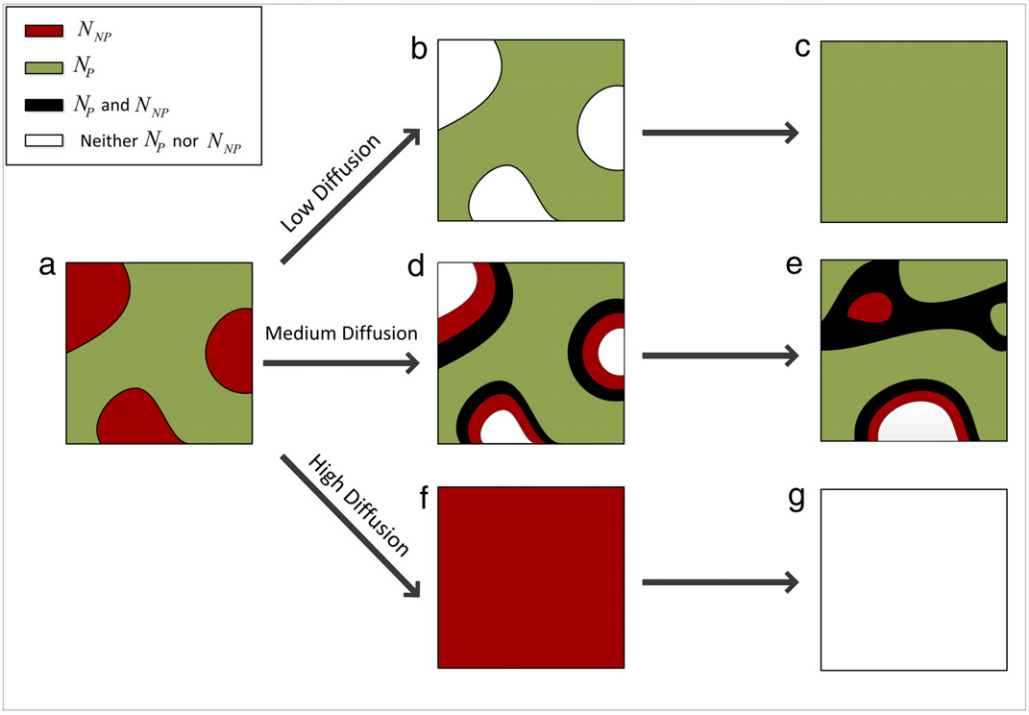


**Fig. 3.** Schematic illustration of the dynamics of spatial distributions in our model. The red area is islands of $N_{NP}$ population. The green area is islands of $N_P$ population. The black areas are areas that include two populations $N_{NP}$ and $N_P$. The white areas are areas that include neither $N_{NP}$ nor $N_P$. (a) We assume a lattice with separate islands of $N_{NP}$ and $N_P$. (b–c) If the diffusion rate of the populations is extremely high, the system will behave as expected in the mean field and the only possible solution is the empty state. (d–e) If the diffusion of the populations is in an intermediate range, the population $N_{NP}$ can continuously take over regions repopulated by $N_P$. (f–g) If the diffusion of the populations is extremely low, only the productive population, $N_P$, can exist. (For interpretation of the references to colour in this figure legend, the reader is referred to the web version of this article.)

two populations become extinct. An interesting feature of these maps is that the diffusion coefficient of $C$ has little effect on the system fate until very fast diffusion where the only solution is extinction. The collapse occurs when the resources are spread out uniformly throughout the lattice, leading to an advantage of $N_{NP}$ over $N_P$ in all lattice sites.

The range of coexistence increases with the resource turnover rate (high $\tilde{\mu}$ values). In order to understand why increasing $\mu$ increases the survival range the mechanism for coexistence must be understood.

## 7. Dynamic mechanism underlying coexistence

To better understand the coexistence dynamics, we change variables and describe the system in terms of the resource, the total producer and non-producer population $N = N_{NP} + N_P$ and the fraction of non-producers in the population $R = \frac{N_{NP}}{N}$. Changing variables in the continuous homogeneous system Eq. (1) leads to the following equations:

$$\begin{cases} \dfrac{dN}{dt} = [(\alpha(C) - \delta) + (\delta - 1)R]\,N \\ \dfrac{dR}{dt} = R(1-R)(\delta - 1) \\ \dfrac{dC}{dt} = \left[\dfrac{\mu}{\nu/(1-R) + N} - k\alpha(C)\right]N. \end{cases} \tag{4}$$

It is seen that $R$ is always increasing, and thus asymptotically will tend to 1, leading to the complete takeover of non-producers in this approximation. However, the rate at which this process proceeds is proportional to $(\delta - 1)$, typically a very small parameter. It is seen from the equations that $N$, $C$ derivatives contain zero-th order terms in this small parameter while the $R$ derivative does not, and thus its dynamics is slow relative to the other variables. We therefore consider in detail the dynamics of invasion of non-producing cells into a region where producers maintain equilibrium with the growth resource.

In the absence of non-producers ($R = 0$), a stable equilibrium is obtained between $C$ and $N$ at $\alpha(C^*) = \delta$ and $N^* = \frac{\mu}{k\delta} - \nu$. In our simulations typically this local population is large ($N^* \approx 100$). The system behaves there as a stable predator–prey system, with oscillatory trajectories around the stable fixed point for most of parameter space, as can be found directly from a stability analysis. (If $k^2\alpha'(C)\,(\nu + N)^2 \geq \mu$, convergence to the stable fixed point is direct and not oscillatory.)

Following an invasion, $R > 0$, the total population $N$ and the resource $C$ decrease, thus decreasing fitness for all; the non-producers "overburden" the group they belong to by their presence (Avilés, 2002). However this happens at rates of order 1, while the fraction $R$ increases at a rate of order $(\delta - 1)$. Since $N_{NP} = RN$, the absolute number of non-producers will decrease even though their fraction increases in the continuous approximation. And since the absolute number of invaders is small, the effect of a decrease in resource, and the consequent decrease in the absolute growth rate, will be more dramatic and their extinction — a likely event. At the same time, the large population of producers will also decrease but will most likely remain far from extinction. The invasion will then fail, and $N_{NP}$ will rapidly fall into its absorbing state, allowing $C$ and $N$ to grow again to their steady state values $C^*$ and $N^*$.

The values $C$ and $N$ can be estimated, assuming that for a limited time $R$ is approximately constant, and following the balance between $N$ and $C$ (i.e. perform an adiabatic approximation in $R$). The two possible solutions are either $N = 0$ or

$$\alpha(C^*) = \delta - (\delta - 1)R, \qquad N^* = \frac{\mu}{k\delta}\,\frac{1}{1 - \frac{(\delta-1)}{\delta}R} - \frac{\nu}{1-R} \tag{5}$$

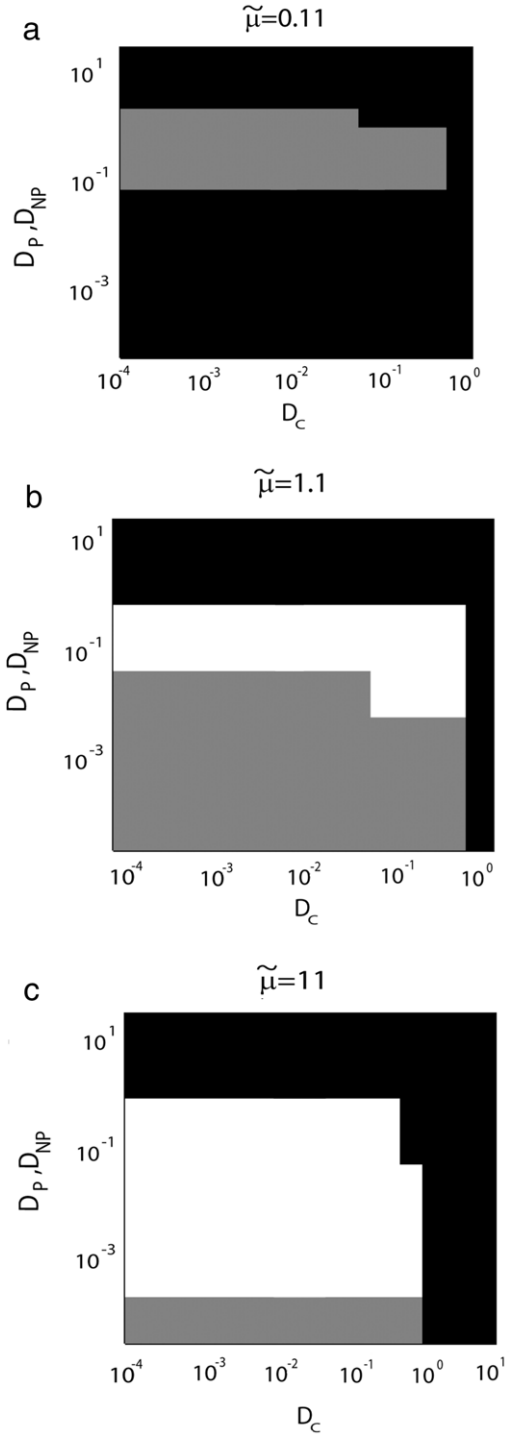


**Fig. 4.** Dependence of system steady state on rate parameters. White — coexistence, gray — only producers survive, black — extinction of both populations. Each panel corresponds to a different value of the resource turnover rate ($\tilde{\mu}$ in Eq. (3)). In each panel the type of steady state is mapped as a function of the resource diffusion rate of $D_C$ ($x$ axis) and cellular diffusion coefficient of the populations, $D_N$, $D_{NP}$ (which is the same in these simulations; $y$ axis). Parameters for all of the simulations are: $\delta = 1.05$, $\tilde{\nu} = 5/11$.

the latter being stable as long as it is positive. The continuous transition to extinction occurs at $R = \frac{\frac{\mu}{\nu k} - \delta}{\left[\frac{\mu}{\nu k} - (\delta - 1)\right]}$ (Fig. 5(a)). If the system were allowed to evolve all the way to this transition, the entire local population would collapse. However, if before this happens the value of $N_{NP} = RN$ is close enough to 1 to have a high probability of it falling to the absorbing state, the system will converge back to its meta-stable state where $R = 0$, and an invasion cycle from a neighboring site can start again.

In order to check that this description is appropriate, we computed the projection of the three-dimensional average flow in the original physical variables, on the two-dimensional planes of variable pairs in the stochastic simulation (Fig. 5(b)–(d)).

Fig. 5(b) shows the flow around the meta-stable point. The grayscale represents the number of sites with a given value of $(C, N_P)$ and the length and direction of the arrows represent the average change between two consecutive time steps starting from that value. This flow is typical of a predator–prey oscillatory flow around the meta-stable fixed point, as expected from the stability analysis above. Fig. 5(c) shows the flow in the $N_{NP} - C$ plane: When $N_{NP}$ is high, consumption of resource exceeds production leading to a decrease in $C$. When $C$ is high it increases $N_{NP}$ since its net growth rate is positive. When $C$ is low, $N_{NP}$ decreases, leading to oscillatory dynamics near the 0 value. When $N_{NP}$ reaches zero $C$ converges to the meta-stable fixed point as in Fig. 5(b). The dynamics for $N_{NP} = 0$ are plotted using a different grayscale since there are many more sites with $N_{NP} = 0$ than with any other value.

The more interesting flow occurs in the $N_{NP} - N_P$ plane (Fig. 5(d)), where both populations decrease until $N_{NP}$ becomes zero and the system flows back to the meta-stable state. One can clearly see a vortex around low values of both populations, but following the extinction of non-producers, producers can grow back and the system is attracted to its steady state of Fig. 5(b).

One way to understand the dynamics is to compare the local dynamics and its timescales to the diffusion timescale. Locally there are two scenarios possible: either the non-producers take over and the entire population becomes extinct, or they start to increase in fraction and then become extinct because of their small absolute number and negative growth rate while the producers survive. Both these processes depend on the local resource concentration. In both cases the producers need to re-establish a local equilibrium with the resource such that the growth rate is positive before a new cycle of invasion can begin; this step depends strongly on the resource turnover rate and serves as a form of "refractory" period.

We can now explain the regions of coexistence in terms of these timescales (Fig. 3). The resource turnover rate, $\tilde{\mu}$ in Eq. (3), affects directly the local cycle time — a small value of $\tilde{\mu}$ induces a long refractory period. If $\tilde{\mu}$ is extremely small, producers can decrease to zero, the resources can stabilize on a sub-threshold value, and the system may reach the marginally stable empty state. From this empty state the local population will grow again only through the diffusion of producers from neighboring sites, and thus a large rate of diffusion is required to support coexistence. However for fast turnover ($\tilde{\mu} \geq 10$), co-existence is ensured as long as the diffusion rate is not much smaller than the time of a local cycle, allowing also smaller diffusion rates. This can be clearly seen in Fig. 3, where the range of coexistence can be seen to shrink drastically to 0, as the value of $\tilde{\mu}$ decreases below a critical value. To summarize, the coexistence mechanism is supported by spatio-temporal patterns that come about through the repeated transition of $N_{NP}$ across its local survival–extinction phase transition. The transition is mediated through a small change in $C$, which in turn tips the balance of growth rate around zero. This results in trajectories that hover around an extinction phase transition of $N_{NP}$. Therefore, we expect to observe a signature of this critical transition in the dynamics; for example the distribution of extinction times – the time between consecutive invasions of $N_{NP}$ in single sites – is expected to be broadly distributed. Fig. 6(a) depicts this distribution as computed from our simulation, showing a long-term power-law decay with a power approximately $-1$ (Bak et al., 1987). This is accompanied by the parallel long range autocorrelation of $N_{NP}$ (Fig. 6(b)).

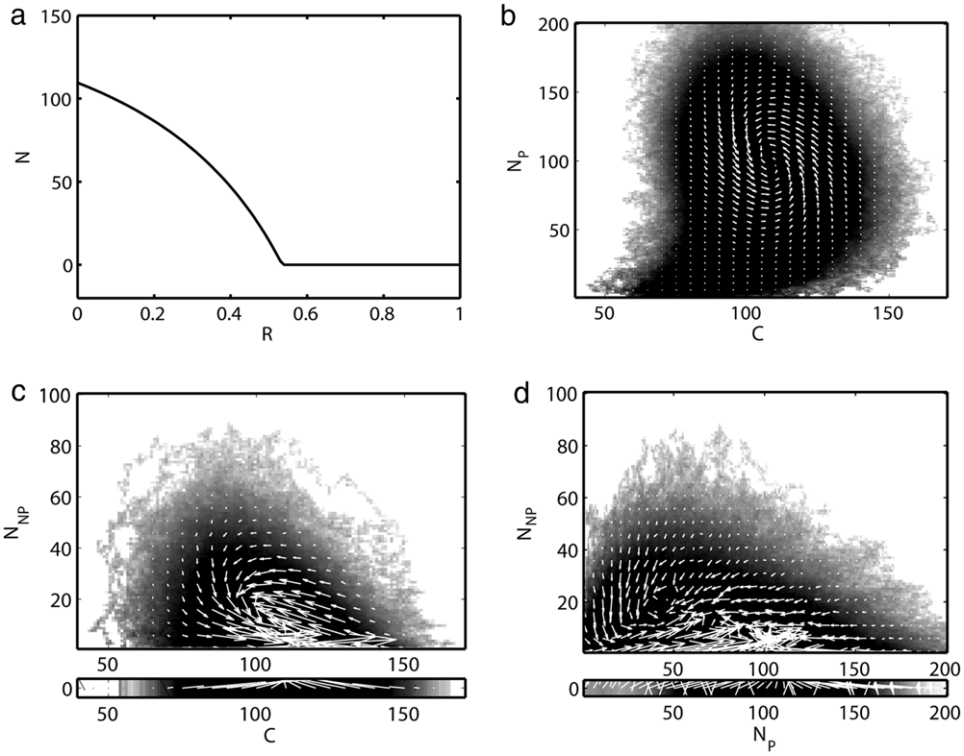


**Fig. 5.** (a) The quasi-steady state of $N$ for a given $R$ value. (b) The flow in the $N_P - C$ plane. The grayscales are probability to be in the given $[N_P, C]$ value. In all subplots, black colors are higher concentration. The grayscales are in a log scale. (c) The flow in the $N_{NP} - C$ plane. The grayscales are probability to be in the given $[N_{NP}, C]$ value. Black colors are higher concentration. The highest concentrations are at the $N_{NP} = 0$ values. (d) The flow in the $N_{NP} - N_P$ plane. The grayscales are probability to be in the given $[N_P, N_{NP}]$ value. The highest concentrations are at the $N_{NP} = 0$ values. The parameters used for all simulations are: $\alpha(C) = 0.01C$, $\delta = 1.05$, $k = 0.5$, $\mu = 110$, $\nu = 100$, $D_C = 10^{-2}$, $D_A = 2 \cdot 10^{-2}$. We artificially separate the strip $N_{NP} = 0$ from $N_{NP} > 0$, since there are many more values for $N_{NP} = 0$ than for any other particular value of $N_{NP} > 0$. We use different scales for the colors and length of arrows for the $N_{NP} = 0$ than for $N_{NP} > 0$ cases.

## 8. Discussion

We have studied a model for cooperation in microorganism populations, taking into account both spatial mobility (diffusion on a lattice) and demographic noise (discrete cells and stochastic reactions). The model is a realization of the public-goods game with particular relevance for active extraction of resource by microbial populations: interactions are indirectly mediated through a dynamic environment; growth rates and production rates are saturating functions; differences between "cooperators" and "defectors" reflect modest changes in phenotype relevant to gene expression for example; and the discreteness of individuals turns out to play an important role in the dynamics. In the continuous limit, either in the mean field or in the reaction–diffusion approximation, the only stable state of the system is total extinction. In marked contrast, the results of our full stochastic simulations show that the model gives rise to coexistence of producing and non-producing cells through the emergence of spatio-temporal patterns in a broad range of parameter space, where diffusion coefficients are intermediate.

This result presents a dramatic case of the qualitative differences in the behavior of discrete stochastic reaction and diffusion models and their PDE/ODE parallel. Such differences were initially studied by Durrett and Levin (1994). We have shown previously many cases of increase in the survival probability of a population following stochastic interactions: e.g. Behar et al. (2013). However, to the best of our knowledge, this is the first presentation of a model where survival is induced by the presence of an absorbing state. As such it represents a novel effect of stochastic interactions.

In terms of pattern formation in nonlinear dynamical systems, our results illustrate an interesting mechanism. Compared to the corresponding continuous spatial model, described by the PDE equation (2), one finds that the continuous model does not exhibit patterns and in particular no Turing instability occurs. Recent work has shown that in PDE systems where Turing instability occurs only in a limited region of parameter space, fluctuations can significantly enlarge this region (Butler and Goldenfeld, 2011). Here we see an example of patterns which have no Turing counterpart in the continuous system, but appear only in the full stochastic system. In particular, no strong asymmetry between the two interacting populations is required, and their diffusion coefficient is in fact taken to be identical in our simulations. A more general understanding and classification of this phenomenon remains an interesting question for further theoretical study (Scott et al., 2011).

From an evolutionary perspective, this model apparently provides another mechanism for assortment of the two competing sub-populations, which is known to allow for coexistence between productive and non-productive phenotypes inhabiting a common environment (Damore and Gore, 2012). However, assortment here does not only break the symmetry of interaction between the competitors; it is reflected also in the asymmetry with respect to the growth-enabling environment. The productive individuals can sustain a local equilibrium with a high density of cells and resource, which turns out to be essential to their resilience to local invasions. These cells hold the local environment at a state which is close to an extinction transition for the non-productive ones; this is where the discreteness of individual becomes important, and the non-producers are driven to dynamic trajectories that locally hover around their extinction transition point.

It should be noted that this effect overcomes the usual mutual exclusion of populations that grow on the same substrate. This is because these populations are not passively consuming the same resource; they are in a two-way interaction with the environment, both consuming and producing it (at least some sub-population).

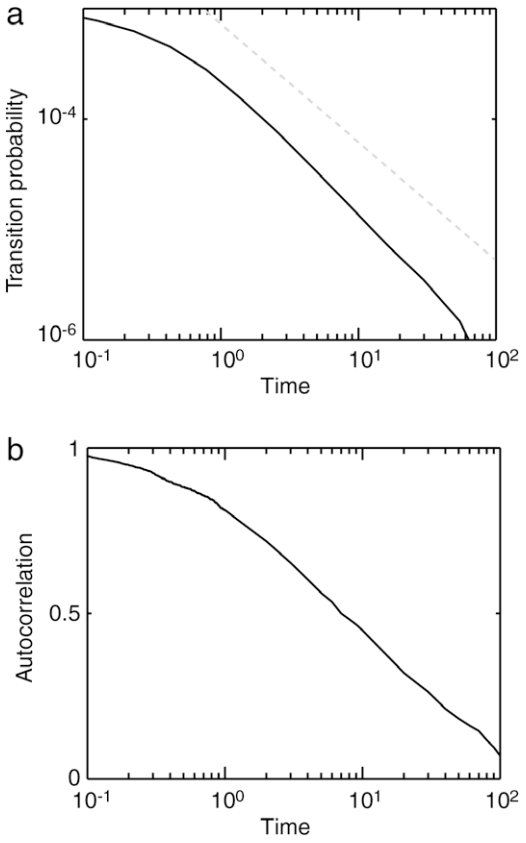


**Fig. 6.** (a) Probability to wait time $T$ before exiting a state of $N_{NP} = 0$ to a non-zero value, (full line) and a $(-1)$ power (dashed gray line). (b) Autocorrelation of $N_{NP}$ as a function of the time delay. This can be clearly observed to decrease logarithmically, after an initial period.

This leads to a more complex behavior as explained above, allowing for long-term coexistence. While extinction of the non-producing species in the entire space is a nonzero event in a finite system, it is exceedingly rare.

The dynamic mechanism underlying the emergence of patterns is related to the vicinity of the system to a critical phase transition, the extinction transition. The concept of criticality is relevant to many ecological systems, both in terms of transitions between different behaviors and in terms of spatio-temporal correlations (Pascual and Guichard, 2005). Ecological models are often formulated in terms of cellular automata with a small number of states; qualitatively different behaviors are identified depending on the existence of delay (or refractoriness) between perturbation and recovery (Greenberg and Hastings, 1978). In contrast, the model studied here derives from differential equations and has an infinitely large number of possible states — the number of cells in a lattice site is discrete but unbounded. The recovery timescale after extinction of one cell type is therefore determined by the linear stability eigenvalues of the partial dynamical system, which can be large or small depending on local parameters. Therefore this system presents a case where different "critical-like" behaviors are observed, interpolating between delayed and non-delayed dynamics.

In most systems described as self-organizing into a critical state, there is an external slow driving force which keeps the system in the vicinity of a phase transition (Dickman et al., 2000). Here, in contrast, the system is driven to reside near a critical point by the interactions between its elements. The slowness is provided by the small differences in the net growth rate of the two microbial subpopulations, corresponding to the notion that gene expression or other phenotypic properties affect global metabolism and growth rate only moderately. Note also that the dynamics can be strongly affected by trajectories hovering around the critical point although it is never actually *at* that point. It is expected that in complex systems with several interacting degrees of freedom such behavior will be found often.

The emergence of spatio-temporal patterns is expected to be observed in experiments. Strains of both yeast and bacteria with defined properties with respect to resource extraction have been developed and studied. Recent work has shown the possibility to grow microbial populations in controlled solid plates with diffusion effects playing an important role in the dynamics (Julou et al., 2013). Parameter space can be examined by changing the plate medium to vary diffusion coefficient, which is an important control parameter in the system. Although our model is simple and realistic systems are expected to display additional complications, the basic effect of coexistence by spatio-temporal patterns may still be found in some experimental realization. We have recently shown that a similar mechanism can affect disease dynamics (Agranovich and Louzoun, 2012). Future experimental and theoretical work is required to advance toward this goal.

## Acknowledgment

This research is supported in part by the Israel Binational Science Foundation personal grant (NB) (grant number 1566/11).

## Appendix A. Supplementary material

Supplementary material related to this article can be found online at http://dx.doi.org/10.1016/j.tpb.2014.06.002.

## References

Agranovich, A., Louzoun, Y., 2012. Predator–prey dynamics in a uniform medium lead to directed percolation and wave-train propagation. Phys. Rev. E 85 (3), 031911.
Agranovich, A., Louzoun, Y., et al., 2006. Catalyst-induced growth with limited catalyst lifespan and competition. J. Theoret. Biol. 241 (2), 307–320.
Alexander, R., 1977. Diagonally implicit Runge–Kutta methods for stiff ODE's. SIAM J. Numer. Anal. 14, 1006–1021.
Alexander, R.D., Borgia, G., 1978. Group selection, altruism, and the levels of organization of life. Annu. Rev. Ecol. Syst. 9, 449–474.
Aparicio, J.P., Solari, H.G., 2001. Population dynamics: Poisson approximation and its relation to the langevin process. Phys. Rev. Lett. 86 (18), 4183–4186.
Avilés, L., 2002. Solving the freeloaders paradox: genetic associations and frequency-dependent selection in the evolution of cooperation among nonrelatives. Proc. Natl. Acad. Sci. 99 (22), 14268–14273.
Axelrod, R., Hamilton, W.D., 1981. The evolution of cooperation. Science 211 (4489), 1390–1396.
Bak, P., Tang, C., et al., 1987. Self-organized criticality: an explanation of the 1/f noise. Phys. Rev. Lett. 59 (4), 381–384.
Behar, H., Agranovich, A., et al., 2013. Diffusion rate determines balance between extinction and proliferation in birth–death processes. Math. Biosci. Eng. 10 (3), 523–550.
Behar, H., Shnerb, N., et al., 2012. Balance between absorbing and positive fixed points in resource consumption models. Phys. Rev. E 86 (3), 031146.
Butler, T., Goldenfeld, N., 2011. Fluctuation-driven Turing patterns. Phys. Rev. E 84 (1).
Carlson, M., Botstein, D., 1982. Organization of the SUC gene family in Saccaromyces. Mol. Coll. Biol. 3, 351–359.
Craig Maclean, R., Brandon, C., 2008. Stable public goods cooperation and dynamic social interactions in yeast. J. Evol. Biol. 21 (6), 1836–1843.
Damore, J.A., Gore, J., 2012. Understanding microbial cooperation. J. Theoret. Biol. 299, 31–41.
Davidovich, H., Louzoun, Y., 2013. The balance between adaptation to catalysts and competition radius shapes the total wealth, time variability and inequality. Eur. Phys. J. B 86 (5), 1–13.
Dickman, R., Munoz, M.A., et al., 2000. Paths to self-organized criticality. Braz. J. Phys. 30 (1).
Doebeli, M., Hauert, C., et al., 2004. The evolutionary origin of cooperators and defectors. Science 306 (5697), 859–862.
Durrett, R., Levin, S., 1994. The importance of being discrete (and spatial). Theor. Popul. Biol. 46 (3), 363–394.
Elhanati, Y., Schuster, S., et al., 2011. Dynamic modeling of cooperative protein secretion in microorganism populations. Theor. Popul. Biol. 80 (1), 49–63.

Eshel, I., 1972. On the neighbor effect and the evolution of altruistic traits. Theor. Popul. Biol. 3 (3), 258–277.
Gore, J., Youk, H., et al., 2009. Snowdrift game dynamics and facultative cheating in yeast. Nature 459 (7244), 253–256.
Greenberg, J.M., Hastings, S., 1978. Spatial patterns for discrete models of diffusion in excitable media. SIAM J. Appl. Math. 34 (3), 515–523.
Hamilton, W.D., 1971. Selection of selfish and altruistic behavior in some extreme models. In: Eisenberg, J.F., Dillon., W.S. (Eds.), Man and Beast: Comparative Social Behavior. Smithsonian Press, Washington, DC, pp. 57–91.
Hanselman, D., Littlefield, B.C., 1997. Mastering MATLAB 5: A Comprehensive Tutorial and Reference. Prentice Hall PTR.
Hauert, C., Holmes, M., et al., 2006. Evolutionary games and population dynamics: maintenance of cooperation in public goods games. Proc. Biol. Sci. 273 (1605), 3131–3132.
Hauert, C., Wakano, J.Y., et al., 2008. Ecological public goods games: cooperation and bifurcation. Theor. Popul. Biol. 73 (2), 257–263.
Hider, R.C., Kong, X., 2010. Chemistry and biology of siderophores. Nat. Prod. Rep. 637–657.
Irwin, A.J., Taylor, P.D., 2001. Evolution of altruism in stepping-stone populations with overlapping generations. Theor. Popul. Biol. 60 (4), 315–325.
Jameson, A., Schmidt, W., et al., 1981. Numerical solutions of the Euler equations by finite volume methods using Runge–Kutta time-stepping schemes. AIAA J. 81, 1259.
Jones, E.W., Pringle, J.R., et al., 1992. Volume II: The Molecular and Cellular Biology of the Yeast Saccharomyces: Gene Expression. Cold Spring Harbor.
Julou, T., Mora, T., et al., 2013. Cell–cell contacts confine public goods diffusion inside pseudomonas aerugniosa clonal microcolonies. Proc. Natl. Acad. Sci. USA 110 (31), 12577–12582.
Kummerli, R., Jiricny, N., et al., 2009. Phenotypic plasticity of a cooperative behaviour in bacteria. J. Evol. Biol. 22 (3), 589–598.
Michod, R.E., Roze, D., 2001. Cooperation and conflict in the evolution of multicellularity. Heredity 86 (Pt 1), 1–7.
Moore, L.S., Stolovicki, E., Braun, E., 2013. Population dynamics of metastable growth-rate phenotypes. PLoS ONE 8 (12), e81671.
Nowak, M.A., 2006. Five rules for the evolution of cooperation. Science 314 (5805), 1560–1563.
Nowak, M.A., Bonhoeffer, S., et al., 1994. Spatial games and the maintenance of cooperation. Proc. Natl. Acad. Sci. USA 91 (11), 4877–4881.
Pascual, M., Guichard, F., 2005. Criticality and disturbance in spatial ecological systems. Trends Ecol. Evolut. 20 (2), 88–95.
Perc, M., Gomez-Gardenes, J., et al., 2013. Evolutionary dynamics of group interactions on structured populations: a review. J. R. Soc. Interface 10 (80), 20120997.
Roberts, G., 2005. Cooperation through interdependence. Anim. Behav. 70 (4), 901–908.
Schuster, S., Kreft, J.U., et al., 2010. Cooperation and cheating in microbial exoenzyme production—theoretical analysis for biotechnological applications. Biotechnol. J. 5 (7), 751–758.
Scott, M., Poulin, F.J., et al., 2011. Approximating intrinsic noise in continuous multispecies models. Proc. R. Soc. A 467 (2127), 718–737.
Stolovicki, E., Braun, E., 2011. Collective dynamics of gene expression in cell populations. PLoS One 6 (6), e20530.
Velicer, G.J., Vos, M., 2009. Sociobiology of the myxobacteria. Annu. Rev. Microbiol. 63, 599–623.
Wakano, J.Y., 2007. Evolution of cooperation in spatial public goods games with common resource dynamics. J. Theoret. Biol. 247 (4), 616–622.
Wakano, J.Y., Hauert, C., 2011. Pattern formation and chaos in spatial ecological public goodsgames. J. Theoret. Biol. 268 (1), 30–38.
Wakano, J.Y., Nowak, M.A., et al., 2009. Spatial dynamics of ecological public goods. Proc. Natl. Acad. Sci. USA 106, 7910–7914.